

A predictive tool to model drug-propellant interactions in pressurized metered dose systems

^{1,2}Jesslynn Ooi, ³Simon Gaisford, ⁴Ben J Boyd, ^{1,2}Paul M Young, *^{1,2}Daniela Traini.

5 ¹Respiratory Technology, Woolcock Institute of Medical Research, 431 Glebe Point Road,
Glebe, NSW 2037, Australia

²Discipline of Pharmacology, Sydney Medical School, The University of Sydney, Sydney
NSW 2006, Australia

³School of Pharmacy, University College London, 29-39 Brunswick Square, London, WC1N
1AX, United Kingdom

10 ⁴Monash Institute of Pharmaceutical Sciences, Monash University, 381 Royal Parade,
Parkville, Victoria 3052, Australia

*To whom correspondence should be addressed

Email: daniela.traini@sydney.edu.au

15

Keywords: Isothermal microcalorimetry, fluorinated interactions, propellant, crystallisation,
pMDI, aerosol science.

Abstract.

20

The purpose of this work was to evaluate gas perfusion isothermal calorimetry (ITC) as a method to characterize the physicochemical changes of active pharmaceutical ingredients (APIs) intended to be formulated in pressurised metered dose inhalers (pMDIs) after exposure to a model propellant. Spray dried samples of beclomethasone dipropionate (BDP) and salbutamol sulphate (SS) were exposed to controlled quantities of 2H,3H-decafluoropentane (HPFP) to determine whether ITC could be used as a suitable analytical method for gathering data on the behavioural properties of the powders in real time. The crystallization kinetics of BDP and the physicochemical properties of SS were successfully characterized using ITC and supported by a variety of other analytical techniques.

25

30

Correlations between real and model propellant systems were also established using hydrofluoroalkane (HFA-227) propellant. In summary, ITC was found to be suitable for gathering data on the crystallization kinetics of BDP and SS. In a wider context, this work will have implications on the use of ITC for stability testing of APIs in HFA-based pMDIs.

1. Introduction

35 Since the introduction of the first commercially available hydrofluoroalkane (HFA)
pressurized metered dose inhaler (pMDI) in 1994(1), significant progress has been made in
understanding the fundamental interactions between active pharmaceutical ingredients (API)
and hydrofluoroalkane propellants, namely HFA 134a and HFA 227. Understanding the
relationship between HFAs and active pharmaceutical ingredients (APIs) used for inhalation
40 formulations is pivotal to the design and performance of the final formulation. Many
techniques have been employed in the past to study API stability in HFAs in terms of
aerodynamic diameter and geometric particle size; including visual inspection of flocculated
particles (2, 3), *in vitro* cascade impaction (4) and *in situ* laser diffraction to study particle
growth (5). High performance liquid chromatography (HPLC) methods have also been
45 utilized to observe chemical stability of APIs exposed to propellants (3). Although previous
studies have provided some insight into the interactions of APIs in this medium, zeta
potential, micelle formation and other physicochemical tests are more challenging to conduct,
due to the volatile nature of HFAs at ambient pressure. To compensate for this shortfall, a
model propellant substitution 2H,3H-decafluoropentane, namely HPFP, which is liquid at
50 ambient pressure, has been proposed to mimic the physiochemical properties of HFA 227 (6).

This model propellant has previously been employed to study drug-HFA interactions. For
example, atomic force microscopy techniques (7-10) have been conducted in which HPFP
was utilised as a medium to further investigate cohesive drug-drug, drug-surfactant, drug-
55 propellant and drug-canister interaction forces. A recent study by Bouhroum (11) has
measured the adhesive forces between beclomethasone dipropionate (BDP) clathrates formed
by trichlorofluoromethane and pMDI components in the presence of HPFP. HPFP has also
been used as a surrogate for HFA to study particle stability of chitosan-sodium
tripolyphosphate nanoparticles intended for the pulmonary delivery of nucleic acids (12).

60 Isothermal calorimetry (ITC) is a quantitative physical technique used to determine reaction
thermodynamics and kinetics. Being invariant to sample physical form, it can be used to
study solutions, solids and heterogeneous mixtures and has been applied to many areas of
pharmaceutical development, including pre-formulation stages of inhalation device
65 development, determination of solubility (13), enthalpy of solution (14), percentage
crystallinity (15) or amorphicity (16) and interactions between drug and carrier (17). The

high sensitivity of the technique means that ITC has potential to study complex drug-propellant interactions, suited to API stability studies (18).

70 Building on previous research (19), this study is designed to expand the use of ITC beyond using water or organic vapours. Specifically, ITC was used to investigate physiochemical changes in API particles after exposure to HPFP. Spray dried samples of BDP and salbutamol sulphate (SS), two common drugs for inhalation with distinctively different properties and solubilities in HFA-227, were eluted with controlled volumes of HPFP to determine whether
75 ITC is suitable for establishing information regarding the crystallization kinetics of inhalation powders in real-time. In a wider context, the studies will have implications for the use of ITC for stability testing in HFA-based pMDIs.

2. Materials and Methods

2.1 Materials.

80 Beclomethasone dipropionate was supplied by Ai Radhe Sales (Gujarat, India). Salbutamol sulphate was supplied by Interchem (Chongqing, China). Water was purified by reverse osmosis (MilliQ, Molsheim, France). All solvents were analytical grade and supplied by Sigma (Sydney, NSW, Australia). Propellant HFA-227 was supplied by Ineos Fluor Ltd. (Cheshire, UK). Metering valves (DF 31, nominal metered volume 50 μ L) and actuators with
85 orifice diameters of 0.3 mm, were supplied by Bepak Europe Limited (Norfolk, UK). Glass pMDI containers were supplied by Saint Gobain plc (London, UK). Aerosol formulations were pressure filled using a Pamasol Laboratory plant 02016 (pamasol W. Mäden AG, Pfäffikon, Switzerland).

90 The model propellant 2H, 3H Decafluoropentane was supplied by Apollo Scientific, Cheshire, UK. This was subsequently purified with chromatographic grade acidic and basic aluminium oxide (Fluka, Gillingham, UK) to remove impurities that could potentially alter measurements (7). Approximately 400 g of acidic aluminium oxide was added to a sealed flask containing 2 L HPFP and agitated using the Ultrasonic Cleaner (Unisonics, Australia)
95 for 45 min. The resultant supernatant was vacuum filtered over a 0.2 μ m PTFE to remove the aluminium oxide. The filtrate was then added to an additional flask containing approximately 400 g of basic aluminium oxide. This secondary mixture was again agitated using the Ultrasonic Cleaner for 45 min and the filtrate removed by vacuum filtration. HPFP was stored in capped laboratory bottles (Boeco, Germany), which contained approximately
100 100g of 2 mm diameter molecular sieves (Sigma-Aldrich, Australia) to prevent moisture ingress.

2.2. Preparation of BDP and SS micro-particulates.

105 Beclomethasone dipropionate and salbutamol sulphate particles were prepared using a Mini Spray Dryer in closed loop configuration (Büchi, B-290, Switzerland). An ethanolic BDP solution (5% w/v) was spray-dried using the following parameters: inlet temperature 60°C, outlet temperature 43°C, feed rate 10% (2.5 mL min⁻¹), 100% aspiration (40 m³.h⁻¹) and an atomizing pressure of 742 kPa. An aqueous salbutamol sulphate solution (10% w/v) was
110 spray dried using the following parameters: inlet temperature 150°C, outlet temperature 95°C,

feed rate 2% (0.5 mL.min⁻¹), 100% aspiration (40 m³.h⁻¹) and atomizing pressure of 742 kPa. The spray dried powders were stored at <10% RH and 25 °C, in tightly sealed containers, for >1 week prior to testing.

115 **2.3. Size Distribution.**

The particle size distributions of both BDP and SS were measured by laser diffraction (Malvern Mastersizer 2000, Malvern, Worcestershire, UK). Approximately 5 mg of dry powder was introduced through a Scirocco dry feeder (Malvern, UK) and dispersed using 4-bar pressure. Samples were measured in triplicate at an obscuration between 3% and 10% with a refractive index of 1.564 and 1.553 for BDP and SS, respectively.

2.4. Scanning Electron Microscopy and Focused Ion Beam Milling.

The BDP and SS micro-particulates were imaged using FEI Quanta 200F (Oregon, USA), field-emission scanning electron microscopy (SEM) prior to and after being suspended in HPFP and HFA-227, respectively. Samples were deposited on sticky carbon tabs, mounted on SEM stubs and sputter coated (Quorum Q150, Kent, UK) on a tilt-rotating stage to achieve a 10 nm gold coating prior to SEM analysis and Focused Ion Beam (FIB) milling. Spray dried particles were then imaged at 5 kV. Focused Ion Beam milling of the samples was performed with a FIB-SEM dual beam system (Quanta 200 3D, FEI, USA). Micro-particulate samples were milled at an accelerating voltage of 30 kV and a beam current of 25 pA. Milling times for all samples were kept under 5 min. The samples were then examined using the SEM at 5 kV and tilted at 30° for visualization of the cross section.

2.5. Specific Surface Area.

The specific surface areas of the BDP and SS micro-particulates were measured using a Micromeritics Tristar II 3020 (GA, USA). Prior to surface area analysis, the samples were degassed with N₂ for 48 hr at 50°C. Approximately 200 mg of sample were used for each experiment. Nitrogen adsorption isotherms were performed at relative pressures between 0.05 and 0.3 at 77.3K and the surface area calculated according to the Brunauer–Emmett–Teller equation.

2.6. Differential Scanning Calorimetry.

Thermal analysis of the BDP and SS micro-particulates, prior to and after 6 hrs exposure to HPFP vapour, was performed using differential scanning calorimetry (DSC Q2000, TA Instruments, Delaware, USA). Approximately 4 mg of sample powder was weighed into non-hermetic T-zero Aluminium pans. All experiments were subject to a heating rate of 10 °C min⁻¹. The cell constant and enthalpy calibrations were performed with indium (Certified Reference Material LGC2601, Batch E1, LGC, London, $T_m = 156.61^\circ\text{C}$, $\Delta H_f = 28.70 \text{ J/g}$) in accordance with the manufacturer's instructions. The measured values were in excellent agreement with those of the reference material ($T_m \pm 0.03^\circ\text{C}$, $\Delta H_f \pm 0.1 \text{ J/g}$). Nitrogen (50 mL min⁻¹) was used as a purge gas and data were analysed with Universal Analysis 2000 software (TA Instruments, Delaware, USA). Approximately 4 mg of each micronized drug was used as a standard to calculate crystalline percentages.

2.7. Isothermal Calorimetry using HPFP.

Calorimetric data was recorded using a 2277 Thermal Activity Monitor (TAM, Thermometric AB, Järfälla, Sweden) at 25°C. Samples of each micro-particulate powder (20 ± 0.01 mg) were weighed directly into the stainless steel calorimetric ampoules. The ampoules were then attached to the gas perfusion accessory, the reservoirs of which had been filled with HPFP (0.9 mL). Mass flow controllers were used to quantitatively mix two gas streams flowing from different sources, one dry nitrogen line and one saturated with HPFP. The relative vapour pressure (RVP) in the sample ampoule could thus be altered in discrete steps (0% for 6 h, 90% for 3 h and finally 0% for 7 h). The immediate and primary advantage of this approach was that the flowing gas could be dry during the loading and equilibration phases; this ensures both that the water content of the sample at the start of each experiment is the same and that no information are lost prior to commencement of data capture. As HPFP was considerably more volatile than traditional solvents, HPFP reservoirs were freshly refilled and the RVP program repeated to assess any irreversible changes to the powder. Data were recorded every 10 s using the dedicated software package Digitam 4.1. Experiments were performed in triplicate and at an amplifier range of 3000 μW. Power-time data was analysed using Origin (Microcal Software Inc., USA).

2.8. Organic Dynamic Vapour Sorption.

Organic Dynamic Vapour Sorption (O-DVS) measurements were performed to study the sorption properties of the powders. Measurements were made with a DVS-1 (Surface

Measurement Systems, UK) at 25 °C using HPFP as the vapour probe. The operational set up of the O-DVS has been previously described (20). Approximately 20 mg of either BDP or SS micro-particulates were weighed into the sample pan and exposed to a three-step HPFP partial pressure cycle of 0% - 90% following a protocol that matched the ITC measurements.

180

2.9. X-Ray Powder Diffraction.

The amorphous structure of the spray dried BDP and SS micro-particulates were characterised using X-ray powder diffraction (XRPD Siemens D6000 diffractometer, Siemens, Karlsruhe, Germany) at a scan range of $5-30^{\circ}2\theta$, step size of 0.04° and count time of 2 s. XRPD was also applied to both powders prior to and post exposure to HPFP vapour for 6 hours.

185

2.10. Fourier Transform Infrared Spectroscopy.

The samples were subjected to Fourier transform infrared (FT-IR) spectroscopy to assess any change in the BDP molecular state after elution with propellant vapour. Samples of BDP were recorded with a PerkinElmer Spectrum 100 FTIR spectrometer in the wavenumber range of $650-4000\text{ cm}^{-1}$ with a resolution of 4 cm^{-1} at ambient conditions.

190

3. Results & Discussion

195

3.1. Physicochemical analysis of the spray-dried model drugs.

Scanning electron microscopy images of the spray dried BDP and SS micro-particles are shown in **Error! Reference source not found.**Figure 1A and B, respectively. The BDP particles had a smooth spherical geometry, with a size ranging from the submicron to around $4\text{ }\mu\text{m}$. In comparison, SEM images of SS showed corrugated spherical particles with a similar size distribution to BDP. In general, the SS morphology appeared to be similar to that reported in previous work, which utilised aqueous solutions to spray dry SS (21, 22); while the spray-dried BDP particles were similar in morphology to that reported by Abdel-Halim et al. (23), wherein particles were prepared from a 20% w/v ethanolic solution . In general, both particulate systems could be considered of a suitable size for inhalation purposes (24), thus making the study of interactions in medical propellants relative to respiratory drug delivery. To study further the internal structure of these particles, focused ion beam microscopy was utilized to ‘dissect’ individual micron sized particles. In general, both particles were found to have a solid internal core

200

205

(**Error! Reference source not found.****Error! Reference source not found.**Figure 1 right
210 panel). This solid internal core was an expected outcome due to the spray drying process,
compared to the alternative technique of spray-freeze drying which can generate particles
with a greater porosity (25, 26).

Particle size distributions of the spray dried BDP and SS micro-particles are shown in **Error!**
215 **Reference source not found.****Error! Reference source not found.**Figure 2 and specific size
parameters described in Table 1. It is important to note that the SS was significantly larger
than BDP, however, both had considerable overlap in the volume of particles between 0.2 μm
and 4 μm . Furthermore both BDP and SS had 100% particles < 10 μm and > 0.2 μm
suggesting that these microparticles were comparable with respect to stability studies in
220 HPFP.

The difference in particle size distribution was further reflected in the apparent specific
surface area, as measured by nitrogen adsorption experiments. The 5-point BET surface areas
for BDP and SS were $4.55 \pm 0.01 \text{ m}^2\text{g}^{-1}$ and $2.10 \pm 0.02 \text{ m}^2\text{g}^{-1}$, respectively, reflecting the
225 geometrically smaller spray dried BDP particles (yielding a surface area approximately 2.2
larger that of the SS particles). Such observations are important since adsorption and
absorption of HPFP onto/into the drug particle is a surface driven phenomenon and should be
taken into consideration when analysing data.

230 **3.2. The influence of HPFP adsorption and absorption on the stability of spray dried BDP micro-particulates.**

After equilibration for 24 hrs in the ampoule, the spray dried microparticles of BDP were
exposed to two cycles at a p/p_0 of 0.9 HPFP. Calorimetric data for the HPFP perfusion of
BDP are shown in **Error! Reference source not found.****Error! Reference source not
235 found.**Figure 3. Analysis of the data suggested that the initial exothermic peak (Cycle 1)
(corresponding to a change in p/p_0 from 0 to 0.9) comprised of heat from three processes
occurring simultaneously: wetting of the internal surfaces of the ampoule, wetting of the BDP
and crystallization of the BDP. Crystallization occurs almost instantaneously, suggesting that
HPFP takes little time to absorb and act as a plasticizer on the powder bed. The enthalpy of
240 crystallisation was obscured by the wetting of the ampoule and sample, as previously
discussed by Ramos et al 2005 (27). Consequently the area under the first endotherm

(corresponding to a change in p/p_0 from 0.9 to 0) can be added to the area under the exotherm to estimate the contribution of crystallization to the initial exotherm. Although the drying of a crystalline sample may not be technically equivalent to the wetting of an amorphous sample, data error can be assumed negligible. Furthermore, assuming a complete and irreversible change in the BDP sample, a second cycle can be used to assess the contribution of vial and powder bed to simple adsorption phenomena.

In both cycles the desorption isotherms were identical, however the average net heat output for the initial exothermic adsorption peak was 4241.4 mJ during cycle 1 and 185.7 mJ during cycle 2, respectively, suggesting an irreversible crystallisation event had occurred in the BDP sample. Furthermore, the peak max occurred earlier in cycle 2 compared with the initial experiment suggesting that time was required for the HPFP to perfuse into the powder bed to drive the increase molecular mobility required for crystallisation.

Whilst the TAM data provides useful information regarding the real-time interaction of fluorinated molecules with BDP, conventional thermal and x-ray data is required to confirm change in the physical state. Subsequently, the thermal responses of the initial spray-dried BDP and TAM samples after exposure to HPFP were studied using DSC and XRPD. Data are presented in **Error! Reference source not found.**Figure 4A and B, respectively. Partial crystallization of BDP was confirmed using DSC. Spray dried BDP exhibited a crystallisation exotherm at 141.47 °C, followed by a melting endotherm at 211.25 °C when heated at a rate of 10 °C min⁻¹ (**Error! Reference source not found.**Figure 4A-i). This finding is in agreement with previous studies (23). In comparison, spray dried BDP that had been exposed to HPFP vapour exhibited a crystallization exotherm at 117.82 °C (**Figure 4A-ii**), followed by a melting endotherm at 212.49 °C. The shift in the temperature at which crystallization occurs and the decrease in the heat of fusion from 46.70 Jg⁻¹ to 17.33 Jg⁻¹ infers that HPFP vapour partially crystallises BDP. Percentage crystallinity (approximately 30.1 %) was calculated by dividing the measured heat of fusion by the melting enthalpy of 100% crystallized BDP (**Error! Reference source not found.**Figure 4A-iii) (28).

X-ray powder diffraction patterns further support evidence of crystallization of BDP by
275 HPFP vapour. The presence of peaks at diffraction angles 9.4°, 11.16°, 12.76°, 14.32°,
15.40°, 16.72°, 18.28°, 19.4°, 19.92° and 23.52° in the XRPD pattern confirms that the raw
material is crystalline BDP (29). A diffuse halo was observed for the spray dried BDP
sample, which confirmed the structure to be predominantly amorphous (23). The peaks for
the spray dried BDP infused with model propellant HPFP were similar to the peaks observed
280 for raw BDP, however additional peaks were observed at 8.08° and 12.32° which could be
attributed to inclusion of HPFP within the crystalline BDP structure (**Error! Reference
source not found.Error! Reference source not found.**Figure 4B-ii). It can be concluded
that the initial exotherm in the TAM is partially due to crystallization of the powder. More
detailed kinetics of the non-aqueous solution mediated transformation from amorphous to
285 crystalline BDP will be achieved in future synchrotron XRPD studies using approaches
recently reported for analogous aqueous solution-mediated transformations (30). It is
interesting to note that crystallization appears to only occur at a surface level through contact
with HPFP vapour (**Error! Reference source not found.Error! Reference source not
found.**Figure 5), which means the heat is produced from partial crystallisation and so the true
290 enthalpy of crystallization cannot be calculated. Some bridging between particles of close
proximity is observed, although the majority of particles maintain their spherical morphology.
It is difficult to ascertain whether surface crystallization impedes further entry of HPFP
vapour into the core of the BDP particle without further investigation. Thus, it can be
inferred from TAM measurements, DSC and SEM that HPFP vapour does crystallize BDP
295 powder, however the mechanism of crystallization appears to be one of surface nucleation.
This crystallisation process is heterogeneous as it forms at the solid/gaseous interface. This
site then acts as a catalyst for further crystallisation.

To further study the interaction of spray dried BDP micro-particles with HPFP model
300 propellant organic dynamic vapour sorption (O-DVS) was utilised. In order to replicate the
ITC experiment, the O-DVS was programmed to match the perfusion method in the TAM
(Figure 3B). It can be seen that following exposure to 90% RVP of HPFP, the mass of the
powder immediately increased by 10%. This is attributed to HPFP adsorption on the surface
of the powder. During the 3 hours period of HPFP elution, an increase in mass gain from 10
305 – 12 % was observed, symptomatic of a process of continued absorption as HPFP infiltrates
to the core of the particle. The process of absorption is seen to continue during the second

period of exposure to HPFP, which implies absorption is not complete for a period of several hours. After the introduction of dry air into the DVS chamber, 2% of mass was immediately lost from the sample, followed by a second slower period of mass loss from 110 % - 106 %.

310 It is proposed that the initial mass loss is due to evaporation of gaseous HPFP from the surface of the BDP, and the secondary mass loss phase due to the gradual displacement of HPFP with nitrogen gas in the internal structure of BDP particles. The second half of the O-DVS cycle is marked by the reintroduction of HPFP into the chamber at 9 hours. Although there is immediate mass gain, the gradient of mass increase is not as pronounced when
315 compared to the first half of the O-DVS cycle. In accordance with this, the re-introduction of nitrogen at 12 hrs results in a similar pattern of mass loss, although less significant than the first O-DVS cycle. This finding can be explained by observing the augmented morphology of the BDP surface. Crystallisation during the first half of the O-DVS cycle can be concluded to have occurred on the particle surface. It is possible that the crystalline surface acts as a
320 barrier towards further HPFP penetration; it is for this reason that less HPFP is absorbed into the internal structure of the BDP particle and subsequently less HPFP released from the structure.

The FTIR spectra of spray dried BDP is in agreement with literature, with major identifying
325 bands occurring at 1730 cm^{-1} and 1754 cm^{-1} , which corresponds to conjugated C=O stretch and C=O stretch for ester groups (Figure 7). A change in the OH vibrational band corresponding to 3474 cm^{-1} appears to sharpen after exposure to HPFP (31), signifying the shift away from OH hydrogen bonded state towards free OH groups (32). In accordance with this the separation of peaks 1751 cm^{-1} and 1712 cm^{-1} indicate a change in carbon bond
330 coupling after HPFP perfusion. However the infrared region between $800 - 1500\text{ cm}^{-1}$ remains largely consistent between samples, with only peaks 1173 cm^{-1} and 1188 cm^{-1} splitting gradually. FTIR spectra thus highlights the bulk of the powder remains largely BDP, with only a fraction of the powder incorporating HPFP into the BDP matrix. These findings suggest that BDP crystallization involves the formation of a clathrate structure.

335

3.3. The influence of HPFP adsorption and absorption on the stability of spray dried SS micro-particulates.

Calorimetric data for HPFP perfusion of SS is shown in Figure 6A. The first exotherm in the
340 initial wetting phase yielded a maximum enthalpy value of 220 μ W, which is due to the
adsorption of HPFP onto the surface of SS and adsorption onto the internal surfaces of the
metal ampoule. When compared against the higher initial enthalpy of BDP, it can be inferred
that there is a distinction between how HPFP interacts with the surface of both APIs. The
initial sharp peak is followed by a wide endotherm, which may be due to immediate HPFP
345 evaporation from the surface of the drug particle, even though the ampoule continued to be
eluted with 90% RVP HPFP. This finding was confirmed by O-DVS (Figure 6B).

In general, a mass loss of more than 1% occurred during elution with nitrogen gas initially,
which can be attributed to water evaporation. When HPFP was introduced, a gain of <1%
350 suggests that HPFP began to displace nitrogen gas and possibly deposit on the surface of the
SS particle. Steady mass loss throughout the period of HPFP perfusion suggests that HPFP
aids in the removal of remaining nitrogen within the amorphous SS particle. During the
second period of nitrogen gas perfusion, all HPFP gas molecules were displaced with
nitrogen and a mass loss of ~2% occurred. The return to baseline is governed by the speed at
355 which nitrogen gas perfuses into the SS particle. The reintroduction of HPFP vapour induced
a repeat of the gas displacement cycle. The second round of HPFP perfusion also produced a
power-time output that retraced the initial round of perfusion, suggesting that the SS did not
undergo any crystallization or chemical change. These observations were further confirmed
by qualitative analysis of SEM images of the SS micro-particulates before and after perfusion
360 with HPFP (Figure 8A and B, respectively) and via X-ray powder (Figure 8C); where dual
broad peaks indicated an amorphous structure typical of spray dried SS (21, 33). Thus
findings from TAM, O-DVS, SEM and XRPD suggest that SS does not readily interact with
gaseous HPFP solvent.

365 **3.4. Characteristics of Powder Suspensions in the ‘real’ propellant HFA-227**

Currently, ITC O-DVS cannot operate with real HFA propellants (either in the gas or liquid
phase). However these techniques may provide a fundamental insight into the interaction of
API micro-particle materials with fluorinated propellants using higher molecular weight
substitutes such as HPFP. To relate the observations reported here, the study additionally
370 evaluated the stability of the spray dried amorphous BDP and SS particulates in a real HFA
system using HFA 227 propellant.

In general, analysis of an HFA 227 pressure filled suspension of spray dried BDP micro-particulates, by SEM, suggested induced time-dependent crystallization (**Error! Reference source not found.****Error! Reference source not found.**Figure 9A-C). Furthermore, crystallization appears to be subject to surface nucleation, as crystallization appears to have occurred instantaneously at multiple surface areas, which were exposed for 6 hours to HFA-227. This particular time dependent sequence captures the process of BDP-solvate compound, namely a clathrate formation (11, 34). The possibility of the formation of a solvated BDP crystal form is likely; DVS data shows an increase in powder mass during solvation of HPFP, which suggests that HPFP solvent molecules interact with BDP molecules and are subsequently trapped inside a clathrate framework (Figure 3B). It is proposed that a similar interaction would occur in the lower molecular weight HFA 227.

In comparison spray dried SS micro-particles maintained their spherical morphology with pitted surfaces after half an hour and 6 hours exposure (see supplementary data). Minimal particle-particle interactions were observed after 6 hours. Such observations match those observed using ITC and O-DVS with HPFP as the model propellant.

390

4. Conclusions

Isothermal calorimetry is a suitable technique to investigate crystallization kinetics of APIs in propellant systems. The early stages of BDP clathrate formation were successfully investigated using a surrogate propellant coupled with ITC. Similarly, the stability of the SS in HFA-227 was predicted using ITC experiments with surrogate propellant. This work establishes ITC as a useful diagnostic tool for predicting API stability in HFA formulations. The use of the ITC could be expanded to include biological and macromolecule preparations intended for pressurized metered dose inhalers.

400

5. Acknowledgements

The research leading to these results has received funding from the European Community's Seventh Framework Programme (FP7/2007-2013) under grant agreement n° 233533. This research was also supported under Australian Research Council's Discovery Projects funding
405 scheme (project number DP120103510). A/Professor Young is the recipient of an Australian Research Council Future Fellowship (project number FT110100996). A/Professor Traini is the recipient of an Australian Research Council Future Fellowship (project number FT12010063). We also thank Asma Buanz for assistance with DSC and Eric Zhu for assistance with focused ion-beam milling.

410

Tables and Figures

Table 1. Average size distributions ($d_{0.1}$, $d_{0.5}$ and $d_{0.9}$) for spray dried SS and spray dried BDP

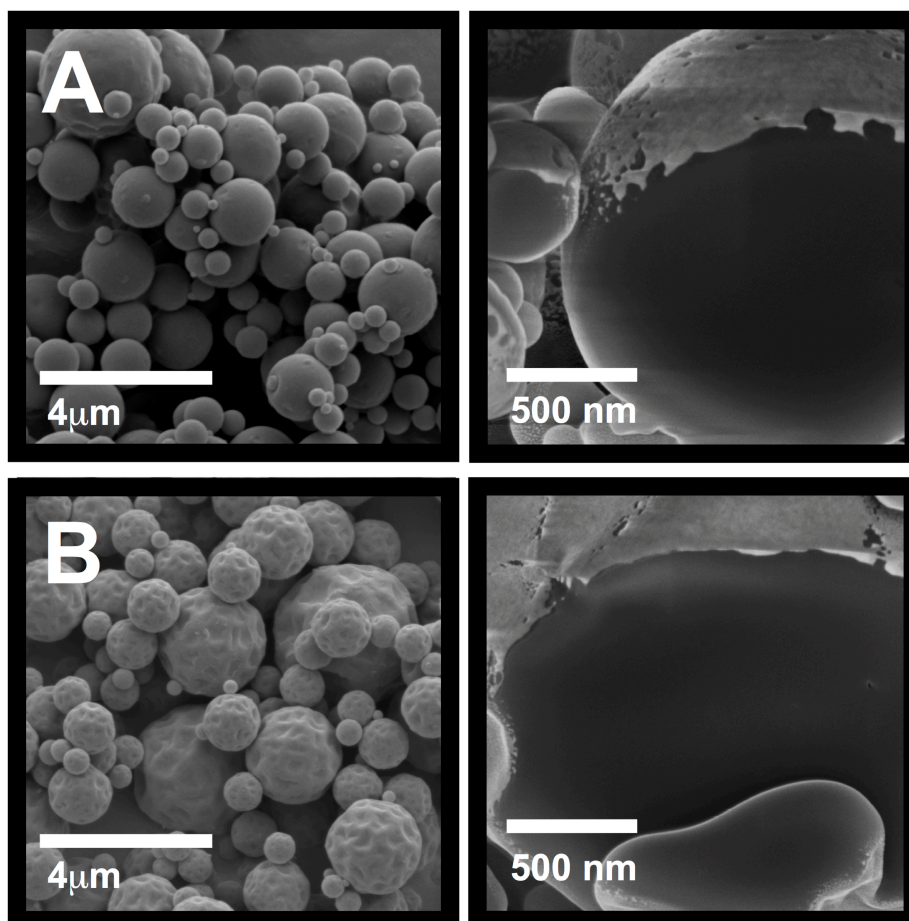
Percentile Value	Beclomethasone Dipropionate ($\mu\text{m} \pm \text{StDev}$)	Salbutamol Sulphate ($\mu\text{m} \pm \text{StDev}$)
$d_{0.1}$	0.62 ± 0.01	0.8 ± 0.02
$d_{0.5}$	1.24 ± 0.01	2.95 ± 0.22
$d_{0.9}$	2.35 ± 0.07	6.12 ± 0.29

415

References

- 420 1. C.L. Leach. Safety assessment of the HFA propellant and the new inhaler. *Eur Res Rev.* 7:35–38 (1997).
2. L. Wu, B. Bharatwaj, J. Panyam, and S.R. da Rocha. Core-shell particles for the dispersion of small polar drugs and biomolecules in hydrofluoroalkane propellants. *Pharm Res.* 25:289-301 (2008).
- 425 3. T.Z. Tzou, R.R. Pachuta, R.B. Coy, and R.K. Schultz. Drug form selection in albuterol-containing metered-dose inhaler formulations and its impact on chemical

and
physical
stability.
Journal of



- pharmaceutical sciences. 86:1352-1357 (1997).
4. E.M. Phillips, P.R. Byron, K. Fults, and A.J. Hickey. Optimized inhalation aerosols. II. Inertial testing methods for particle size analysis of pressurized inhalers. *Pharm Res.* 7:1228-1233 (1990).
- 435 5. S.A. Jones, G.P. Martin, and M.B. Brown. High-pressure aerosol suspensions--a novel laser diffraction particle sizing system for hydrofluoroalkane pressurised metered dose inhalers. *International journal of pharmaceuticals.* 302:154-165 (2005).
6. P.G. Rogueda. HPFP, a model propellant for pMDIs. *Drug Dev Ind Pharm.* 29:39-49
- 440 7. D. Traini, P. Rogueda, P. Young, and R. Price. Surface Energy and Interparticle Force Correlation in Model pMDI Formulations. *Pharm Res.* 22:816-825 (2005).

8. D. Traini, P.M. Young, R. Price, and P. Rogueda. A Novel Apparatus for the Determination of Solubility in Pressurized Metered Dose Inhalers. *Drug Dev Ind Pharm.* 32:1159-1163 (2006).
445
9. D. Traini, P.M. Young, P. Rogueda, and R. Price. Investigation into the influence of polymeric stabilizing excipients on inter-particulate forces in pressurised metered dose inhalers. *International journal of pharmaceutics.* 320:58-63 (2006).
10. P.G. Rogueda, R. Price, T. Smith, P.M. Young, and D. Traini. Particle synergy and aerosol performance in non-aqueous liquid of two combinations metered dose inhalation formulations: an AFM and Raman investigation. *J Colloid Interface Sci.* 361:649-655 (2011).
450
11. A. Bouhroum, J.C. Burley, N.R. Champness, R.C. Toon, P.A. Jinks, P.M. Williams, and C.J. Roberts. An assessment of beclomethasone dipropionate clathrate formation in a model suspension metered dose inhaler. *International journal of pharmaceutics.* 391:98-106 (2010).
455
12. K. Sharma, S. Somavarapu, K. Taylor, and N. Govind. PEG-Based Positively Charged Nanoparticles for Pulmonary Delivery of Nucleic Acids, *Drug Delivery to the Lung*, Edinburgh, 2008.
13. G. Castronuovo, V. Elia, M. Niccoli, and F. Velleca. Simultaneous determination of solubility, dissolution and dilution enthalpies of a substance from a single calorimetric experiment. *Thermochimica Acta.* 320:13-22 (1998).
460
14. R. Chadha, N. Kashid, and D.V.S. Jain. Microcalorimetric studies to determine the enthalpy of solution of diclofenac sodium, paracetamol and their binary mixtures at 310.15 K. *Journal of Pharmaceutical and Biomedical Analysis.* 30:1515-1522 (2003).
465
15. D. Gao and J.H. Rytting. Use of solution calorimetry to determine the extent of crystallinity of drugs and excipients. *International journal of pharmaceutics.* 151:183-192 (1997).
16. S. Gaisford. Isothermal microcalorimetry for quantifying amorphous content in processed pharmaceuticals. *Advanced Drug Delivery Reviews.* 64:431-439 (2012).
470
17. G.R. Lloyd, D.Q.M. Craig, and A. Smith. A calorimetric investigation into the interaction between paracetamol and polyethylene glycol 4000 in physical mixes and solid dispersions. *European Journal of Pharmaceutics and Biopharmaceutics.* 48:59-65 (1999).
18. S.J. Charlebois, A.U. Daniels, and G. Lewis. Isothermal microcalorimetry: an analytical technique for assessing the dynamic chemical stability of UHMWPE. *Biomaterials.* 24:291-296 (2003).
475
19. H. Ahmed, G. Buckton, and D. Rawlins. The use of isothermal microcalorimetry in the study of small degrees of amorphous content of a hydrophobic powder. *International journal of pharmaceutics.* 130 195-201 (1996).
480
20. P.M. Young, H. Chiou, T. Tee, D. Traini, H.-K. Chan, F. Thielmann, and D. Burnett. The Use of Organic Vapor Sorption to Determine Low Levels of Amorphous Content in Processed Pharmaceutical Powders. *Drug Dev Ind Pharm.* 33:91-97 (2007).
21. A. Chawla, K.M.G. Taylor, J.M. Newton, and M.C.R. Johnson. Production of spray dried salbutamol sulphate for use in dry powder aerosol formulation. *International journal of pharmaceutics.* 108:233-240 (1994).
485
22. A. Columbano, G. Buckton, and P. Wikeley. Characterisation of surface modified salbutamol sulphate-alkylpolyglycoside microparticles prepared by spray drying. *International journal of pharmaceutics.* 253:61-70 (2003).
23. H. Abdel-Halim, D. Traini, D. Hibbs, S. Gaisford, and P. Young. Modelling of molecular phase transitions in pharmaceutical inhalation compounds: An in silico approach. *European Journal of Pharmaceutics and Biopharmaceutics.* 78:83-89 (2011).
490

24. T.C. Carvalho, J.I. Peters, and R.O. Williams, 3rd. Influence of particle size on regional lung deposition--what evidence is there? *International journal of pharmaceuticals*. 406:1-10 (2011).
495
25. L. Qian and H. Zhang. Controlled freezing and freeze drying: a versatile route for porous and micro-/nano-structured materials. *Journal of Chemical Technology & Biotechnology*. 86:172-184 (2011).
26. Y.-F. Maa, P.-A. Nguyen, T. Sweeney, S. Shire, and C. Hsu. Protein Inhalation Powders: Spray Drying vs Spray Freeze Drying. *Pharm Res*. 16:249-254 (1999).
500
27. R. Ramos, S. Gaisford, and G. Buckton. Calorimetric determination of amorphous content in lactose: a note on the preparation of calibration curves. *International journal of pharmaceuticals*. 300:13-21 (2005).
28. G.d.C. Vasconcelos, R.L. Mazur, E.C. Botelho, M.C. Rezende, and M.L. Costa. Evaluation of crystallization kinetics of poly (ether-ketoneketone) and poly (ether-etherketone) by DSC. *J Aerosp Technol Manag*. 2:155-162 (2010).
505
29. L.-M. Xu, Q.-X. Zhang, Y. Zhou, H. Zhao, J.-X. Wang, and J.-F. Chen. Engineering drug ultrafine particles of beclomethasone dipropionate for dry powder inhalation. *International journal of pharmaceuticals*. 436:1-9 (2012).
- 510 30. J. Boetker, T. Rades, J. Rantanen, A. Hawley, and B.J. Boyd. Structural elucidation of rapid solution-mediated phase transitions in pharmaceutical solids using in situ synchrotron SAXS/WAXS. *Molecular pharmaceuticals*. 9:2787-2791 (2012).
31. Z. Wang, J.F. Chen, Y. Le, Z.G. Shen, and J. Yun. Preparation of ultrafine beclomethasone dipropionate drug powder by antisolvent precipitation. *Ind Eng Chem Res*. 46:4839-4845 (2007).
515
32. J.P. Coates. The interpretation of infrared spectra: Published reference sources. *Appl Spectrosc Rev*. 31:179-192 (1996).
33. D.O. Corrigan, O.I. Corrigan, and A.M. Healy. Physicochemical and in vitro deposition properties of salbutamol sulphate/ipratropium bromide and salbutamol sulphate/excipient spray dried mixtures for use in dry powder inhalers. *International journal of pharmaceuticals*. 322:22-30 (2006).
520
34. J.A. Harris, M.D. Carducci, and P.B. Myrdal. Beclomethasone dipropionate crystallized from HFA-134a and ethanol. *Acta Crystallographica Section E*. 59:o1631-o1633 (2003).
525